JOURNAL OF AIRCRAFT
Vol. 43, No. 2, March–April 2006

Free-to-Roll Investigation of the Preproduction F/A-18E Powered-Approach Wing Drop

D. Bruce Owens*
NASA Langley Research Center, Hampton, Virginia 23681
Elaine M. Bryant†
U.S. Air Force/University of Maryland, College Park, Maryland 20742
and
Jewel B. Barlow‡
University of Maryland, College Park, Maryland 20742

A free-to-roll study of the low-speed lateral characteristics of the preproduction F/A-18E was conducted in the NASA Langley 12-Foot Low-Speed Tunnel. In developmental flight tests the F/A-18E unexpectedly experienced uncommanded lateral motions in the power-approach configuration. The objective of this study was to determine the feasibility of using the free-to-roll technique for the detection of uncommanded lateral motions for the preproduction F/A-18E in the power-approach configuration. The data revealed that this technique in conjunction with static data revealed insight into the cause of the lateral motions. The free-to-roll technique identified uncommanded lateral motions at the same angle-of-attack range as experienced in flight tests. The cause of the uncommanded lateral motions was unsteady asymmetric wing stall. The paper also shows that free-to-roll data or static force and moment data alone are not enough to accurately predict and characterize uncommanded lateral motion.

Nomenclature

C_L = lift coefficient
C_l = total rolling-moment coefficient
C_{lo} = rolling-moment forcing function coefficient
C_{lp} = dynamic lateral stability coefficient, roll damping
$C_{l\beta}$ = static lateral stability coefficient, spring effect
α = angle of attack
β = angle of sideslip
ϕ = body-axis roll angle

I. Introduction

IN 1996 the U.S. Navy's F/A-18E/F Super Hornet experienced uncommanded lateral motions, or wing drop, in the power-approach (PA) configuration during developmental flight tests. These motions were not expected based on computational or experimental predictions during the design studies. Wing drop posed a potential risk to flight safety because of its occurrence at low altitudes and airspeeds. Based on data from investigative flight tests, wing drop was eliminated by retracting deployable vents located on the leading-edge extension (LEX). The vents were located at the junction of the LEX and the wing. Figure 1 shows the location of the LEX and the LEX vent in the open position. Aligning the LEX vent flush with the LEX generates a LEX vents-closed configuration. Although the LEX vents are not employed on the production version of the Super Hornet, several efforts have been made to understand how opening the vents changed the flow topology that resulted in the uncommanded motions.

Although closing the LEX vents eliminated the wing-drop problem, questions remained as to the occurrence and cause of the phenomenon and how the vents-open configuration played a roll. References 1–4 report studies of the flow topologies on preproduction F/A-18E models that have shed much light on the characteristics of the flows. Cook[1] conducted an in-depth study into the behavior of the flow over the preproduction F/A-18E. He determined that the phenomenon was characteristic of a subcritical flow bifurcation, "the abrupt replacement of an unstable flow topology with a stable one."[2] Cook[1] concluded from flow-visualization tests that opening the vents lifted the LEX vortices away from the wing surface and pushed them toward the fuselage. The result was a separated region at midwing, which prevented the snag vortex from properly forming. This, in turn, would cause the outboard portion of the wing to separate. Off-surface flow visualization and wake surveys showed that this phenomenon was asymmetric and unsteady.

The time dependence of forces and flows that were observed and reported by Cook were with stationary models. In actual flight events, the airplane exhibited transient motions in response to force and moment variations caused by wing flow unsteadiness. This experience provided a strong motivation for the application of the free-to-roll (FTR) method. The classical FTR test technique would offer additional light on the flight dynamics and aerodynamics of the lateral motions of the preproduction, powered-approach F/A-18E configuration. The technique shows the response of the aircraft model to time-dependent forces and moments, static, and dynamic lateral stability. Owens et al.[5,6] reported on an extensive study of transonic uncommanded lateral motions of military aircraft using the free-to-roll technique, including the preproduction F/A-18E. The motivations, methods, and objectives for the application of the FTR method to the PA configuration parallel those for the transonic FTR tests of the preproduction F/A-18E. The physics of the aerodynamic phenomena associated with the uncommanded motions in the two cases are different.

The objective of the current effort was to conduct a FTR feasibility test on the preproduction F/A-18E to determine if this technique can be used to detect the uncommanded lateral motions as seen in flight. The method of evaluation was to compare indications for uncommanded lateral motions from the FTR method to the results from the in-flight tests (Table 1) and the static data.[1–4] Good correlation between the developmental flight testing and the FTR testing, supported by static testing, would help establish capability for early

Presented as Paper 2005-0239 at the 43rd Aerospace Sciences Meeting and Exhibit, Reno, NV, 10–14 January 2005; received 25 March 2005; revision received 8 June 2005; accepted for publication 9 June 2005.

*Aerospace Engineer, Flight Dynamics Branch. Associate Fellow AIAA.
†Graduate Student, Aerospace Engineering. Member AIAA.
‡Director, Glenn L. Martin Wind Tunnel, Aerospace Engineering. Associate Fellow AIAA.

Table 1 Value of α and β when PA wing drop occurred for the given flight maneuver

Aircraft, flight, maneuver	α, deg	β, deg
E1, 12,19	15.0	0.0
E2, 17, 67	12.1	−0.4
E1, 26, 18	15.8	0.2
E1, 26, 20	15.0	0.7
E2, 39, 13	14.5	0.5
E2, 39, 21	13.6	−2.5
E2, 39, 23	13.8	1.2
E2, 39, 24	13.7	0.0
E2, 40, 41	13.3	−1.2
F1, 06, 12	14.2	Unavailable

Fig. 1 F/A-18E Super Hornet in approach configuration with the LEX vents open.

identification of potential uncommanded lateral motions. In support of this method of evaluation, a FTR figure of merit (FOM) developed in Ref. 5 was used to quantify the severity of model motion, and assessments were carried out in three areas: severity and types of model motions, unsteady and nonlinear aerodynamics, and roll damping.

II. Experimental Approach

The model used for both the static and the FTR testing was a 10% scale model of the preproduction F/A-18E. The model, constructed of balsa wood, plywood, fiberglass, and aluminum, was outfitted with wing-tip missiles, canopy, engine inlets, leading-edge flaps (LEF), ailerons, flap shrouds, trailing-edge flaps (TEF), vertical tail, horizontal tail (HT), and LEX vents. The control surfaces were movable and could be set at specific values. For the data presented herein the HTs and rudders were set to 0 deg. The LEX vents could be set to various open positions, or they could be closed completely. The static and FTR testing were both done in the NASA Langley 12-Foot Low-Speed Tunnel. The experiments were conducted at sea-level pressure and density with a freestream dynamic pressure of 4 psf resulting in a mean aerodynamic chord-based Reynolds number of 0.5×10^6. Although numerous configurations were tested, the paper will present LEX vents closed and LEX vents open with the LEF = 10 deg, TEF = 30 deg, and ailerons = 30 deg (symmetric trailing-edge-down deflection). This positioning of the ailerons and TEF is referred to as the PA half-configuration.

A. Static Testing

The static force and moments were measured using an internally mounted six-component strain-gauge balance (NASA FF12). A series of both α and β sweeps were conducted with the configurations. Initially α sweeps over the range $-4 \text{ deg} \le \alpha \le 20$ deg were conducted, but for the majority of the runs a smaller α-range ($10 \text{ deg} \le \alpha \le 20$ deg) with a higher resolution was chosen to cover the area of interest. Also, β sweeps with a range of $-16 \text{ deg} \le \beta \le 16$ deg were performed in the smaller α range to assess the static lateral characteristics. The data were sampled at a rate of 80 Hz for 10 s using a low-pass analog filter with cutoff frequency of 4 Hz. All data taken during the 10-s sample time were recorded. The paper will present both the time-averaged balance data as well as the time history of the rolling-moment balance signal over this 10-s window.

B. Free-to-Roll Testing

In the FTR test technique the model was constrained to roll about the longitudinal body axis. Switching from the static-force-and-moment phase to the FTR required replacing the balance with the FTR rig. The FTR rig houses a resolver to measure the roll-angle time history with an accuracy of 0.12 deg. The roll-angle signal was recorded at a rate of 200 Hz using a low-pass analog filter with a cutoff frequency of 4 Hz. Video of the lateral activity was also recorded. The FTR rig contained an air brake to stop the motion and allow the data point to start with a zero initial roll rate. The model's mass was balanced such that the lateral and vertical center-of-gravity coordinates were located on the roll axis. The model's roll inertia was determined experimentally and found to be 0.40 slug-ft^2. This inertia value is close to that required for dynamic scaling. With knowledge of the roll inertia, the total rolling moment C_l can be calculated by twice differentiating the roll angle signal. The rolling-moment time histories were then used in parameter-identification (PID) methods to determine C_{lp}. The PID method used is described in Ref. 5.

There were three ways to conduct a FTR test point: continuous pitch sweeps, pitch-pause, and bank and release. For the continuous pitch sweeps, the model was allowed to roll freely while going through a range of pitch angles. This type of test point quickly revealed any lateral activity over the α range. The procedure for a pitch-pause point involved setting the model to the desired α and holding it there with the brake. Upon brake release the lateral motion was recorded. The information gathered reveals what the model will do when the roll angle and the roll rate are set to zero. The procedure for the bank and release points was to set the model at an initial roll angle other than zero and then release the brake. The bank and release points were used to assess how the model will react to a given initial rolling moment, assess roll damping for the cases where no lateral activity existed at a pitch-pause point, and investigate how inducing a rolling motion affects any motions observed previously.

To quantify the lateral activity, a FOM was used similar to the one developed by Owens et al.[5,6] The FOM is calculated from the roll-angle time histories and captures amplitude and rate effects. It is defined by $p_{P-V} \equiv (|\Delta\phi/\Delta t| b/2V_\infty)_{\max}$. The plots of the FTR–FOM vs α were used to quantify the relative severity of the lateral activity for various configurations and test conditions. This FOM is not intended to indicate the type of motion, how long it took for the motion to develop, or how often the events happened. However it has proven to be an accurate indicator of where uncommanded lateral motion will occur in flight[5] and serves as conservative first filter for assessing the severity of the motion.

The rolling motion can be described by a combination of a forcing function C_{lo}, roll damping C_{lp}, and static lateral stability $C_{l\beta}$ effects. The equation of motion for the FTR test technique is:

$$I_x\ddot{\phi}/qSb + C_{l_{\dot\phi}}(\dot\phi b/2V_\infty) + C_{l_\phi}\phi = C_{\text{lo}}$$

This equation is analogous to a mass-spring-damper system where C_{lo} represents an aerodynamic forcing function; C_{l_ϕ} represents the spring constant, which, along with the inertia, determines the frequency of oscillation; and $C_{l_{\dot\phi}}$ represents the damping coefficient. In the FTR technique, the use of $C_{l_{\dot\phi}}$ andC_{lp} is kinematically equivalent. In the analysis to follow, the equation of motion will be used to highlight the aerodynamic parameters that caused the rolling motion. Exact solutions to the equation of motion are not being sought. Along this vein, C_{lo} will be discussed only as an initial forcing function because an accurate quantification over the range of roll angles was not obtained. Also, $C_{l\beta}$ will be used in place of C_{l_ϕ} because C_{l_ϕ} could not be measured directly. The FTR technique captures the composite effect of both static and dynamic forces acting on the model regardless of whether they are steady or unsteady. The FTR roll-angle time histories presented are solely open-loop motions caused by aerodynamics because all control surfaces are fixed. In a full-scale aircraft the control system is used to correct the rolling

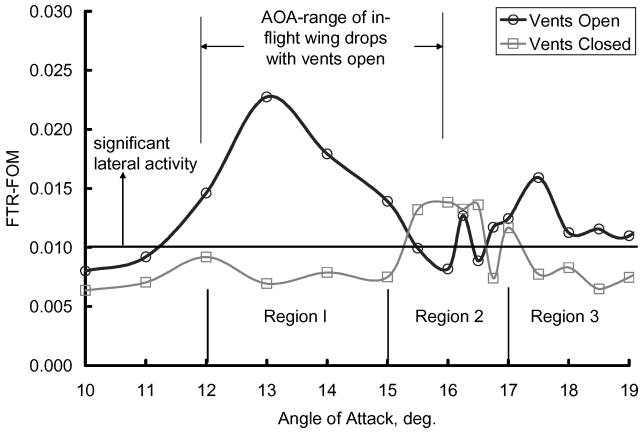

Fig. 2 FTR-FOM comparison between vents closed and vents open. Values of the FOM are calculated using pitch-pause points.

motions. Therefore, the FTR technique cannot be used directly to predict aircraft motions.

III. Results and Analysis

This section will discuss the results for the vents-open and vents-closed configurations. The analysis will begin by using the FTR–FOM to show the relative severity and α ranges of lateral activity for the configurations. Then detailed analysis will be presented for representative points within the α range of lateral activity. The lateral activity of the two configurations is compared in Fig. 2 using the FTR–FOM. The plot shows that for 12 deg $\leq \alpha \leq$ 15 deg opening the vents caused a significant increase in lateral activity with the maximum activity being at $\alpha = 13$ deg. This α range directly correlates to the α range in flight tests where wing drop occurred[5] (Table 1). (Note: the horizontal line drawn at $p_{p-v} = 0.010$ is a subjective dividing line between insignificant and significant lateral activity.) The value was set at 0.010 based on the amount of lateral activity the model exhibited in the low-angle-of-attack, attached flow region. For $\alpha = 15.5$, 16, and 16.5 deg, closing the vents increased lateral activity relative to the vents-open position. For $\alpha = 16.25$ and 17 deg, the severity of lateral activity was the same for both positions of the vents. For $\alpha = 16.75$ and $\geq$17.5 deg opening the vents caused an increase in lateral activity. In summary, the FTR–FOM plot divides the α range into three regions: 12 deg $\leq \alpha \leq$ 15 deg, 15.5 deg $\leq \alpha \leq$ 17 deg, and $\alpha >$ 17 deg. For regions 1 and 3 there is a distinct reduction in lateral activity by closing the vents. In region 2 there are mixed results.

The following discussion will use the FTR–FOM plot as the starting point for more detailed analysis. The points that will be analyzed will be one from region 1 and one from region 2 because this covers the α range, where wing drop was seen in flight. From region 1, $\alpha = 13$ deg is chosen for analysis because this point shows the largest difference between vents open and closed, and wing drop was first identified in flight at $\alpha = 13$ deg (Ref. 3). To show the amplitude and frequency change of the lateral activity between the two configurations, the roll-angle time histories are shown for vents open and closed in Fig. 3. The plot reiterates the large reduction in lateral activity by closing the vents. The cause of the rolling motion can be generated by any or all combinations of a forcing function C_{lo}, spring effects $C_{l\beta}$, and roll damping C_{lp}. Also, the aerodynamic terms can be unsteady. The following discussion will address each of these possibilities.

The time-averaged values of C_{lo} are shown in Fig. 4 with a plot of rolling-moment coefficient from the static force and moment test. (Note. There is an average $C_l = 0.002$ offset for both configurations below $\alpha = 17$ deg. The cause of this asymmetry in the data is probably a result of tunnel sidewash and/or model asymmetries. The data will be discussed relative to the offset.) The time-averaged value of C_{lo} at $\alpha = 13$ deg for the vents-open configuration is not large enough to initiate a significant rolling motion. Therefore, the balance time-history signals must be observed to determine if a forcing

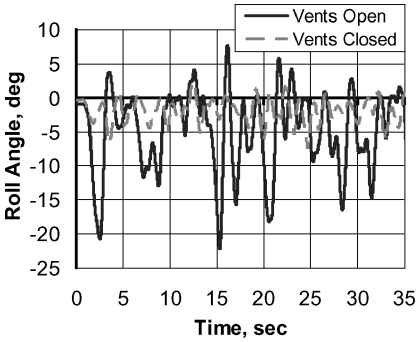

Fig. 3 Roll-angle time histories for the vents-open and –closed configurations at $\alpha = 13$ deg.

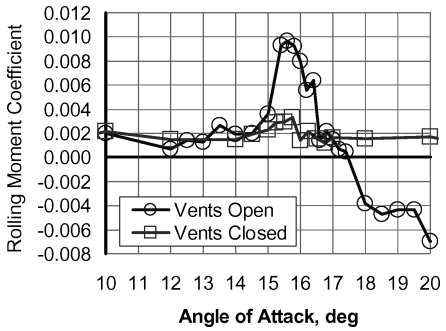

Fig. 4 Effect of vents on the time-averaged static balance rolling moment at $\beta = 0$ deg.

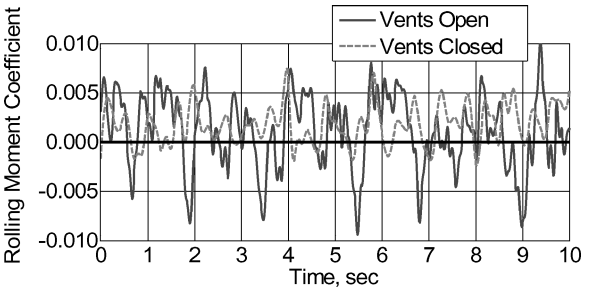

Fig. 5 Balance rolling-moment time history for vents open and vents closed at $\alpha = 12$ deg and $\beta = 0$ deg.

function exists that would initiate rigid-body motion. The balance rolling-moment time-history signals for the $\alpha = 12$ deg data in Fig. 4 is shown in Fig. 5 for the vents-open and -closed position. No balance data were taken for the vents-closed case at $\alpha = 13$ deg, and so a comparison is made at $\alpha = 12$ deg. The characteristics of the balance signals at $\alpha = 12$ deg are indicative of the balance signals where data were taken in the 12 deg $\leq \alpha \leq$ 15 deg for the two configurations. The plot shows that the vents-open configuration had aperiodic rolling moment spikes with sufficient amplitude and low enough frequency that would probably initiate rigid-body rolling motion, whereas, although the vents-closed configuration had an unsteady rolling moment, the amplitude was much smaller. Figure 6 shows the static lateral stability characteristics $C_{l\beta}$ for the vents-open configuration. The plot shows that the model had a strong spring $C_{l\beta}$. The roll damping characteristics, calculated using the PID method mentioned earlier, are shown in Fig. 7. The data from pitch-pause and bank and release points were used in the PID calculations. The plot shows that the model was damped, and no significant difference or change in roll damping characteristics over the α range where activity was seen in flight. Therefore, based on the spring-mass-damper analogy, the lateral activity produced by opening the vents in the $12 \leq \alpha \leq 15$ deg range was caused by an unsteady forcing function of sufficient amplitude. The response to this forcing function was wing drops because the model is well damped with a strong restoring force (spring).

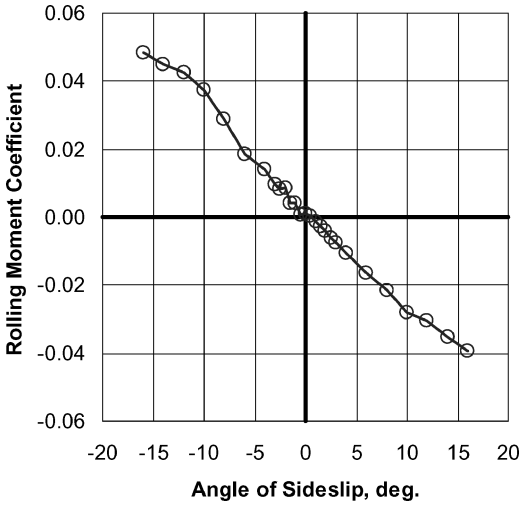

Fig. 6 Static lateral stability characteristics for the vents-open configuration at $\alpha = 13$ deg.

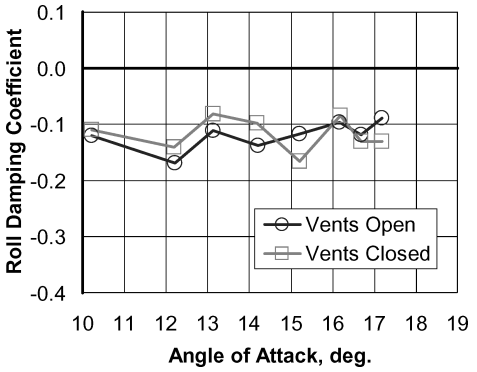

Fig. 7 Effect of vents on roll damping at $\beta = 0$ deg.

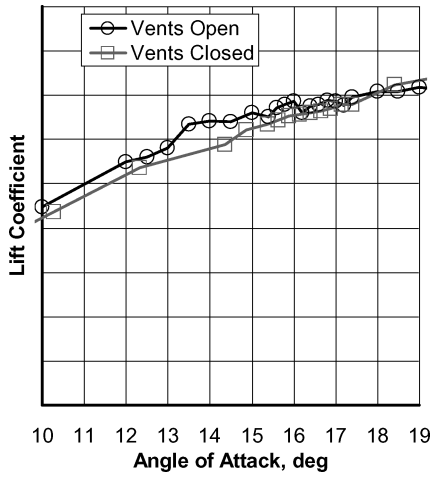

Fig. 8 Lift characteristics for the vents-open and vents-closed configurations at $\beta = 0$ deg.

The lift characteristics of the two configurations are shown in Fig. 8. The plot shows there were no dramatic breaks in lift. These data show that even though no time-averaged rolling-moment spike occurred (Fig. 4) and no significant changes in the time-averaged lift-curve slope were evident (Fig. 8), the wing can still experience an unsteady aerodynamic forcing function that causes uncommanded lateral motions. It is then left to the FTR technique to show that this unsteady aerodynamic forcing function produces undesirable lateral activity.

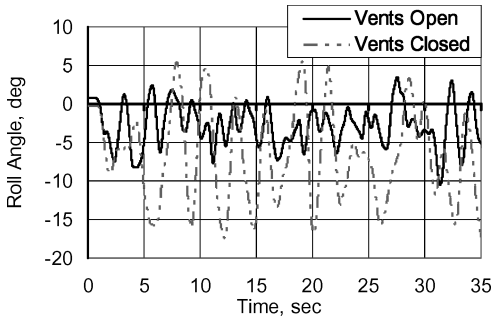

Fig. 9 Roll-angle time histories of the vents-open and vents-closed configurations at $\alpha = 16$ deg.

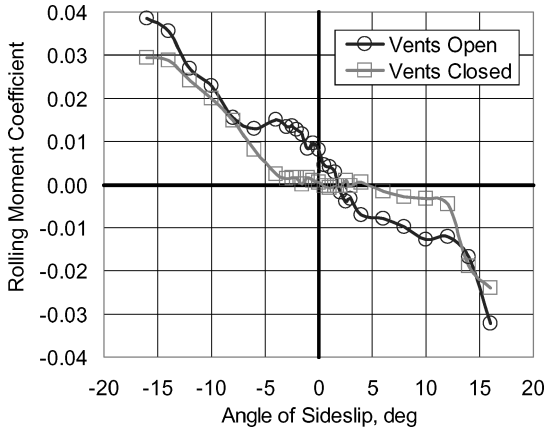

Fig. 10 Static lateral stability for vents open and closed at $\alpha = 16$ deg.

From region 2, the lateral activity at $\alpha = 16$ deg will be analyzed because this occurs at a rapid change in the slope of the static rolling-moment curve of Fig. 4 and is the point in region 2 where the lateral activity between the two configurations is a maximum as indicated by the FTR–FOM plot of Fig. 2. The roll-angle time histories of the vents-closed and -open positions are shown in Fig. 9. Prior to the FTR testing, it was expected that the vents-open position would exhibit significant wing drop at α around 16 deg because the wing is going through stall and there is a significant spike in the rolling-moment curve (Fig. 4). The wing stall (Fig. 8) and rolling-moment characteristics (Fig. 4) are benign for the vents-closed configuration. Therefore, it was expected that the vents-closed configuration would not exhibit significant lateral activity. Figure 9 shows with a plot of the roll-angle time histories that just the opposite happened. Compared to vents-open activity at $\alpha = 13$ deg, the vents-closed activity at $\alpha = 16$ deg is of smaller amplitude and higher frequency.

The time-averaged value of the C_{lo} shown in Fig. 4 shows that at $\alpha = 16$ deg there is a significant value of C_{lo} (0.006) for the vents-open case. The roll-angle time-history plot for the vents-open configuration (Fig. 9) shows a left-wing-down bias, in contrast to the right-wing-down rolling-moment data of Fig. 4. Previous data[3] show that this same 10% F/A-18E model can exhibit negative rolling-moment spikes. Evidently, when the model was changed from the static force and moment mount to the FTR the model had a tendency to stall such that a left-wing-down rolling moment was generated as in the previous test of Ref. 3.

The static lateral stability at $\alpha = 16$ deg is shown in Fig. 10 with a plot of C_l vs β. The plot shows that the vents-open configuration is stable in the -4 deg $\leq \beta \leq +4$ deg range with a C_{lo} of 0.008. This value equals the C_{lo} in Fig. 4. The trim point is around $\beta = 1.75$ deg. This is close to the average value of β that corresponds to the average roll angle in Fig. 9 assuming the possibility that the vents-open curve of Fig. 9 can be reflected about the origin. Figure 10 shows that the vents-closed configuration is neutrally stable with a zero-rolling-moment value for -4 deg $\leq \beta \leq +4$ deg. Therefore any disturbance in the flow will cause the model to roll within this β range. Figure 11

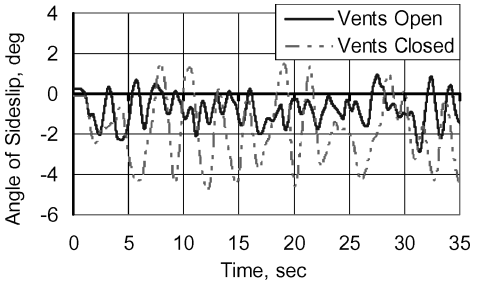

Fig. 11 β time histories from the free-to-roll data of the vents-opens and -closed configurations at $\alpha = 16$ deg.

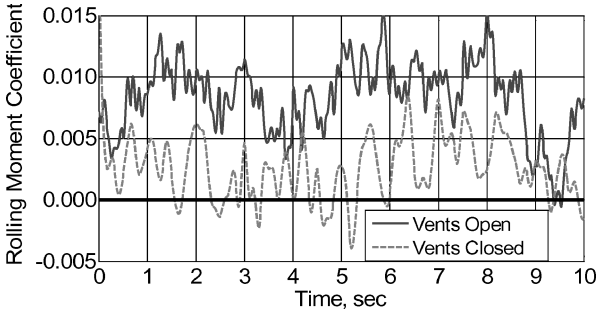

Fig. 12 Balance rolling-moment time history for vents open and vents closed at $\alpha = 16$ deg and $\beta = 0$ deg.

shows that the β range for the vents-closed roll-angle time history in Fig. 9 is also approximately within $-4 \text{ deg} \leq \beta \leq +4$ deg. The roll damping at $\alpha = 16$ in Fig. 7 shows that the model is well damped for both configurations.

Now investigating the possibility of an unsteady forcing function, Fig. 12 compares the balance rolling-moment time history of the vents open to vents closed at $\alpha = 16$ deg. Figure 12 shows that both vents-open and vents-closed configurations exhibited unsteady rolling-moment variations—though at reduced levels than seen in the earlier data for $\alpha = 12$ deg. The frequency of the rolling-moment variations for the vents-closed configuration is lower than the vents open. For the case of the vents-closed configuration, the neutral static lateral stability at small β allowed the unsteady rolling moment to significantly roll the model. The stable $C_{l\beta}$ characteristic of the vents-open configuration provides a strong restoring force, which decreases the impact of the relatively small unsteady rolling moments (Fig. 12) on motions of the model (Fig. 9), while still exciting small motions about the trim roll angle. The data show that neither the static lateral stability nor the presence of unsteady aerodynamic rolling moments by themselves predict the motion of the model. The FTR testing shows the impact of the combinative effects of static stability, damping, and unsteady aerodynamic forces.

The analysis has shown the benefits of the FTR technique in assessing uncommanded lateral activity. Using only roll-angle time histories, expressed as a figure of merit, the FTR technique rapidly gives the angle-of-attack range, where significant lateral activity will occur and discernment of configuration effects. Although the detailed analysis at $\alpha = 13$ and 16 deg showed that the static balance data alone might indicate potential for significant uncommanded lateral activity, it is only the FTR technique that shows the integrated effects of an initial forcing function and static and dynamic stability. Although the roll damping characteristics could be obtained from a proper forced oscillation method, the FTR technique inherently assesses roll damping. A new aircraft program would, after their initial stability and control testing, conduct a FTR test to quickly assess any potential for unacceptable lateral activity. This would also allow the aircraft program to have an early quantification of roll damping without using the forced oscillation technique. If the tested configurations do exhibit undesirable lateral activity, then fixes to the configuration could be accomplished during the FTR test. Now that specific points of significant lateral activity are known, detailed balance information could also be extracted from the prior static force and moment test to assist in understanding the cause of the lateral activity. Conducting a detailed analysis of the balance time histories during the initial stability and control testing would probably be too time consuming given the cost and time schedules of a typical wind-tunnel test. Therefore, this analysis has shown the value in coupling a static force and moment test with the FTR technique to more quickly and accurately capture the lateral activity characteristics.

IV. Conclusions

The FTR technique was used to assess the potential for a preproduction F/A-18E model to predict wing drop as was experienced in flight. Using a FTR–FOM, the technique accurately captured the α range, where wing drop was experienced in flight. Also, the technique showed that, in agreement with flight data, lateral activity was significantly reduced if not eliminated by closing the LEX vents. In the $\alpha = 12$ to 15 deg range, the analysis of the FTR and static force and moment data showed that the lateral activity with the vents open was caused by an unsteady aerodynamic forcing function. The response to this forcing function was wing drops because the model is well damped with a strong lateral stability restoring force. The lift characteristics and time-averaged static rolling-moment values showed no obvious indication for wing drop in this α range. This result shows the importance in using the FTR technique along with unsteady force and moment measurements to predict areas of uncommanded lateral motions. In the $15 \text{ deg} < \alpha < 17$ deg range, the lateral activity of the vents-closed case was primarily caused by neutral static stability with contribution from an unsteady forcing function. In this α range for the vents-open case, the lift characteristics and time-averaged static rolling-moment values would indicate a potential for wing drop. The FTR technique showed that the model would just roll over to trim out the rolling-moment spike and then wing rock with a low amplitude and rate about this trim point probably because of an unsteady forcing function. Roll damping was found to be stable for all configurations. This research has shown that coupling a static force and moment test with the FTR technique more quickly and accurately captures the lateral activity characteristics of the preproduction F/A-18E in the PA configuration.

Acknowledgments

The authors would like to thank Steve Cook and Steve Donaldson of NAVAIR, Patuxent River, Maryland, for research guidance and financial sponsorship.

References

[1]Cook, S., "On Flow Topology Changes Accompanying Aerodynamic Bifurcation for Aircraft with Vented Strakes," Ph.D. Dissertation, Dept. of Aerospace Engineering, Univ. of Maryland, College Park, May 2003.

[2]Cook, S., and Barlow, J., "An Investigation of Low-Speed Lateral Characteristics of a Simplified F/A-18E Configuration," AIAA Paper 2003-0931, Jan. 2003.

[3]Cook, S., and Barlow, J., "Investigation of Effects of Leading Edge Extension Vents the Lateral Characteristics of the F/A-18-E in Power Approach Configuration," AIAA Paper 2000-4510, Aug. 2000.

[4]Cook, S., and Barlow, J., "Investigation of Critical States of the F/A-18E in Power Approach Configuration Using Mini-Tuft Flow Visualization," AIAA Paper 2001-4145, Aug. 2001.

[5]Owens, B., Capone, F., Hall, R., Brandon, J., and Chambers, J., "Transonic Free-To-Roll Analysis of Abrupt Wing Stall on Military Aircraft," *Journal of Aircraft*, Vol. 41, No. 3, 2004, pp. 474–484.

[6]Owens, B., McConnell, J., Brandon, J., and Hall, B., "Transonic Free-To-Roll Analysis of the F/A-18E and F-35 Configurations," AIAA Paper 2004-5053, Aug. 2004.